Smoothed Particle Inference Analysis of SNR DEM L71

Vikram Dwarkadas[1], Kari Frank[2], Jared Siegel[1], Aldo Panfichi[1], Ryan Crum[3], David Burrows[3]

[1]University of Chicago, [2]Northwestern, CIERA,[3]Penn State University

INTRODUCTION

Elements beyond H and He are fused in the cores of massive stars, and dispersed into the surrounding medium when the stars core-collapse as a supernova (SN). The thermonuclear deflagration of a white dwarf in a binary system can lead to a Type Ia SN. In either case, the SN explosion leads to a highly supersonic shock wave propagating outwards, heating the plasma to millions of degrees, and causing it to emit in X-rays. The expanding shell of gas and dust will form supernova remnants (SNRs) that live for thousands of years. The intricate 3-dimensional morphology of a SNR can lead to significant variation in spectral properties across the face of the remnant as well as along the line-of-sight. X-ray observations of SNRs typically provide relatively few photons to investigate these complex structures, thus making it a challenging endeavor to accurately measure the physical conditions throughout the entire volume.

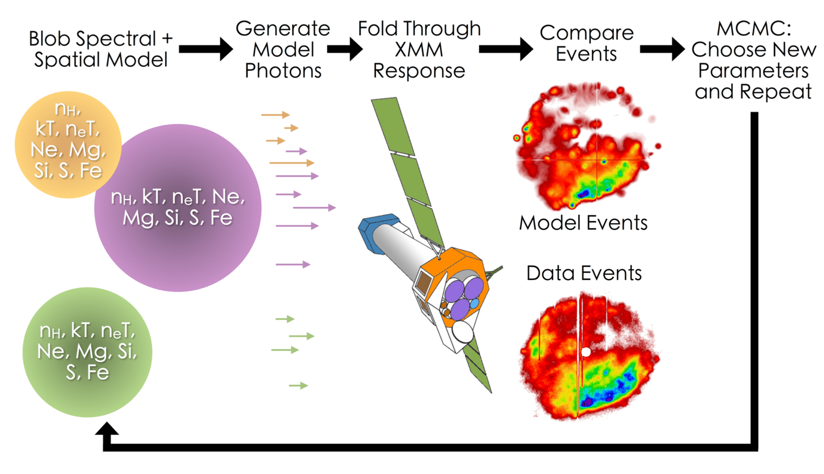

Figure 1: Flowchart of the SPI fitting process.

Smoothed Particle Inference

Smoothed Particle Inference (SPI [Peterson et al. 2007]) takes advantage of both the spatial and spectral information available in the data. SPI models the plasma as a collection of independent 'smoothed particles,' or blobs. Multiple blobs can occupy the same line of sight, or the same space, providing the ability to model a multiphase plasma. No particular morphology or symmetry is assumed, allowing the blob model to reproduce any arbitrary spatial-spectral distribution. SPI forward-folds the blob model through the *XMM-Newton* instrument to predict detector positions and energies for each model photon. The resulting model and observed data are compared, new model parameters chosen accordingly, and the process iterated on till convergence is reached.

SPI Analysis of SNR DEM L71

We apply SPI to SNR DEM L71, a ~4400 year old SNR in the LMC. DEM L71 has been previously classified as a Type Ia remnant due to an enhanced Fe abundance in the center (Hughes et al. 2003; van der Heyden et al. 2003).

We use a vpshock spectral model to describe the emission from each blob, with absorbing column density, temperature, ionization age, and O, Ne, Mg, Si, S, and Fe abundances, as free parameters. The model includes 50 blobs, each of which can vary independently in size and position. Convergence results in a reduced χ^2 of 1.15.

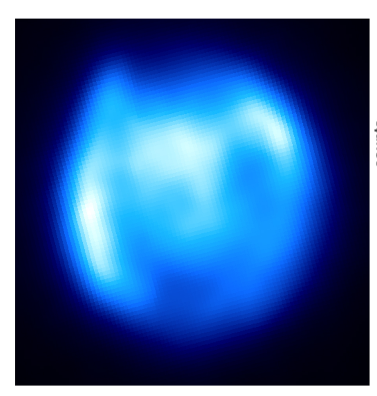

Figure 2: Combined EPIC-pn and MOS exposure-corrected image in 0.2–8.0 keV band.

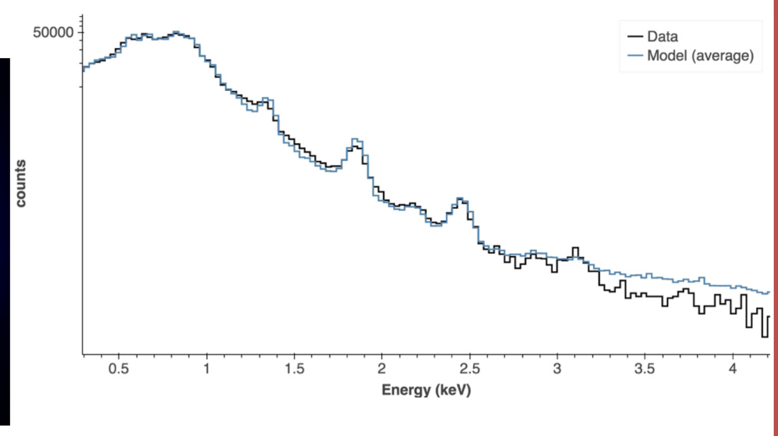

Figure 3: Best fit model spectrum (blue) compared to the observed spectrum (black) for DEM L71.

Isolating the Ejecta

Selection Criteria:

1. Blob kT > 1.0 keV
2. Blob Fe > 1.0 $Fe_\odot$
3. Blob Radius < 26"

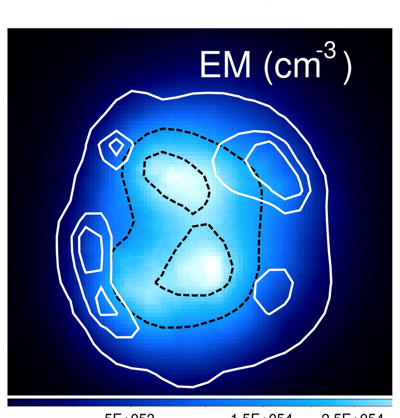

Figure 7: Ejecta EM (cm^{-3}) map, square root scale. Black - Ejecta EM contours. White - overall EM contours.

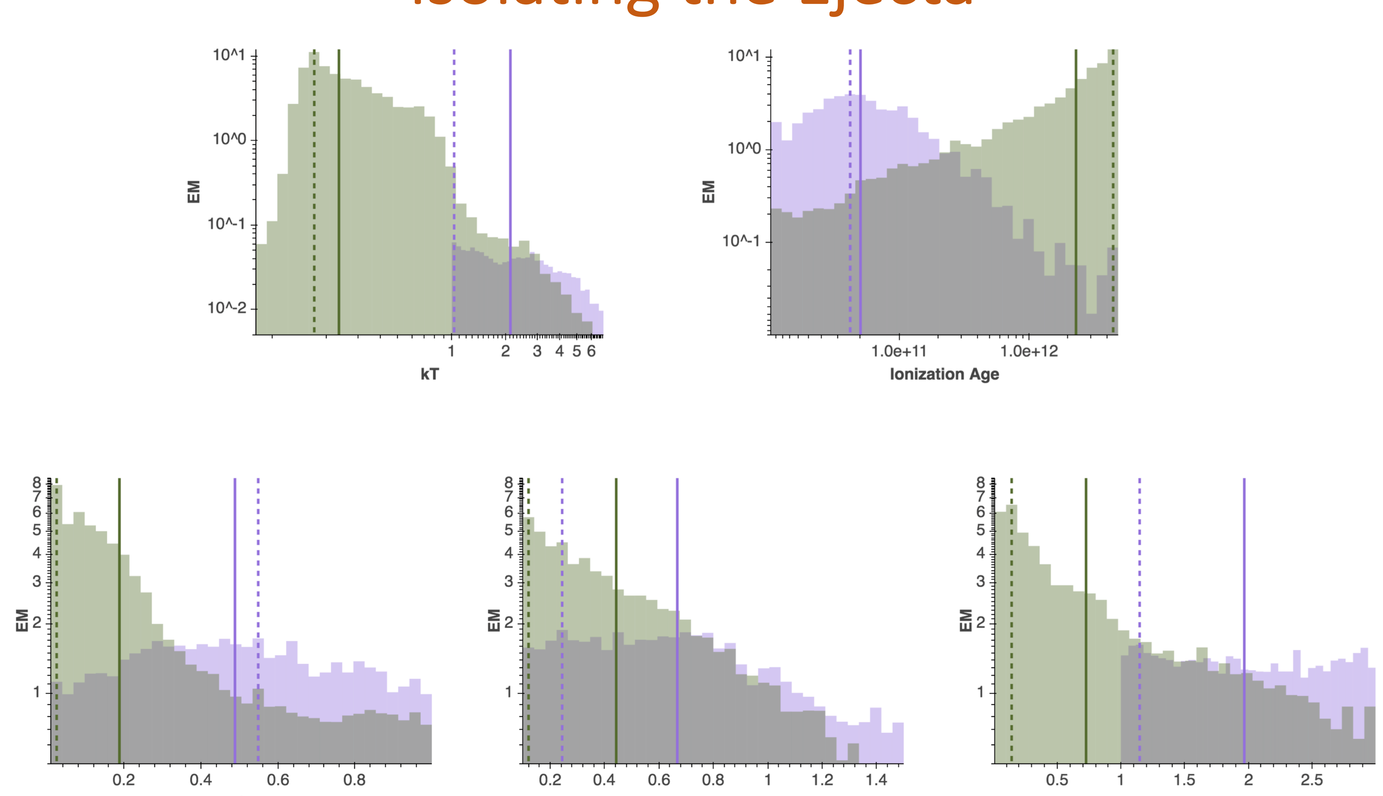

Figure 8: EM-weighted parameter distributions for the ejecta (purple) and swept-up medium (green). Dashed lines - Mode of the Distribution. Solid lines - Median. Except for temperature (kT), ejecta have been scaled up by factor of 40.

Identifying the Contact Discontinuity

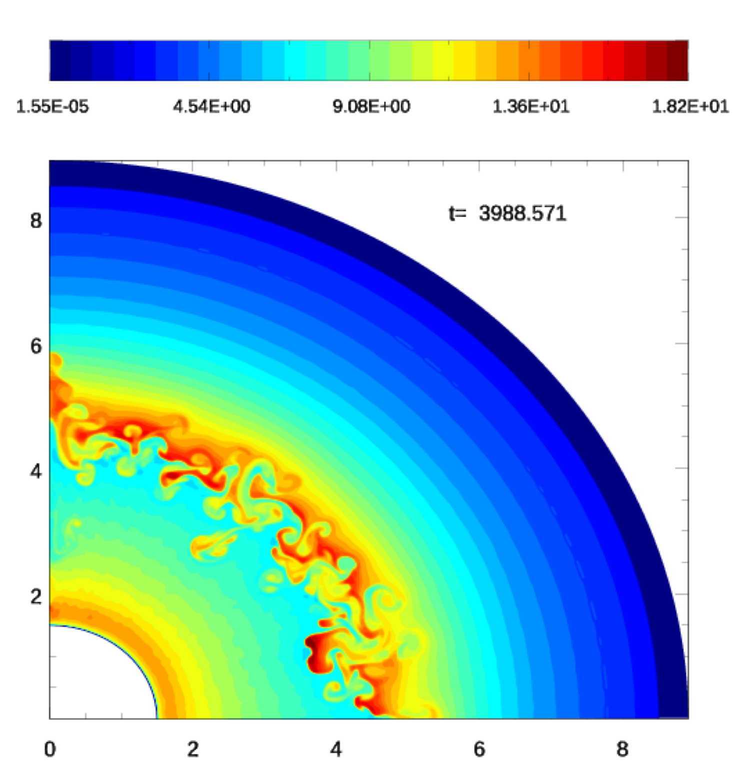

Figure 9: Filled contour plot of gas temperature (keV) within the remnant at an age of 3988.6 yr. From a 2D simulation of DEM L71 carried out using the VH-1 code (Frank et al. (2019)). The contact discontinuity (CD) is unstable to the Rayleigh-Taylor (R-T) instability. The effect of the instability is to spread the CD over a wide region, > 10% of the remnant radius. This leads to a considerable variation in temperatures in the region of the CD. Thus we would expect the standard deviation of temperature to be maximum around the CD.

Radius where maximum standard deviation in temperature is seen corresponds nicely with radius of contact discontinuity.

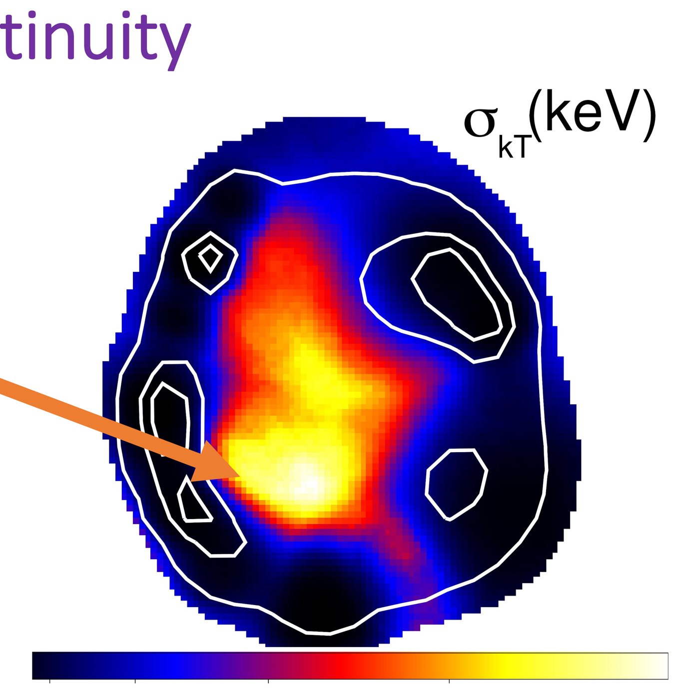

Figure 10: EM-weighted standard deviation of the temperature on a square root scale, with EM contours

Parameter Maps

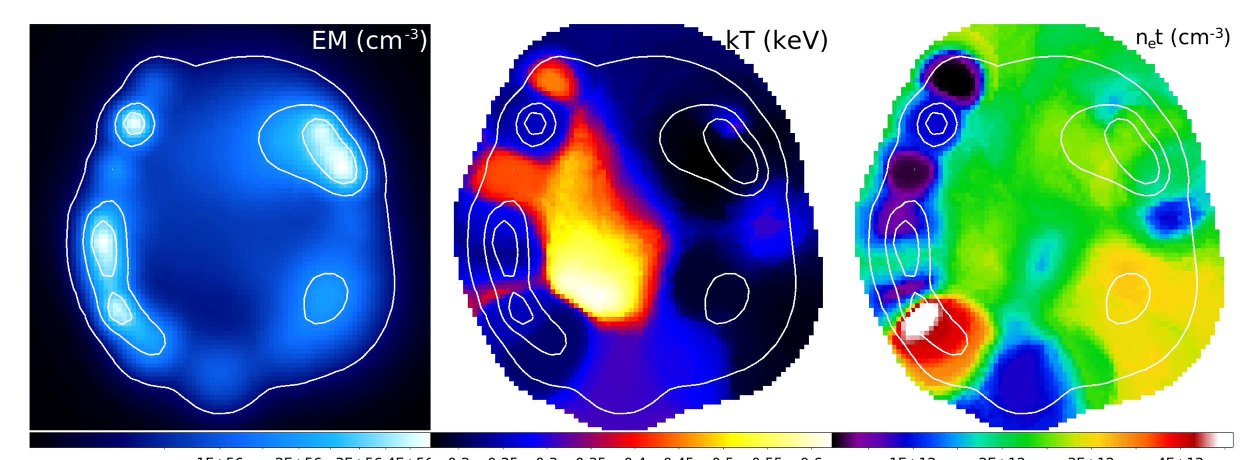

Figure 4: (*Left*) Total Emission-Measure (EM; cm^{-3}), square root scale; (*Center*) Median EM Weighted Electron Temperature (keV); (*Right*) Median EM Weighted Ionization Age $(\mathrm{cm}^{-3} s)$.

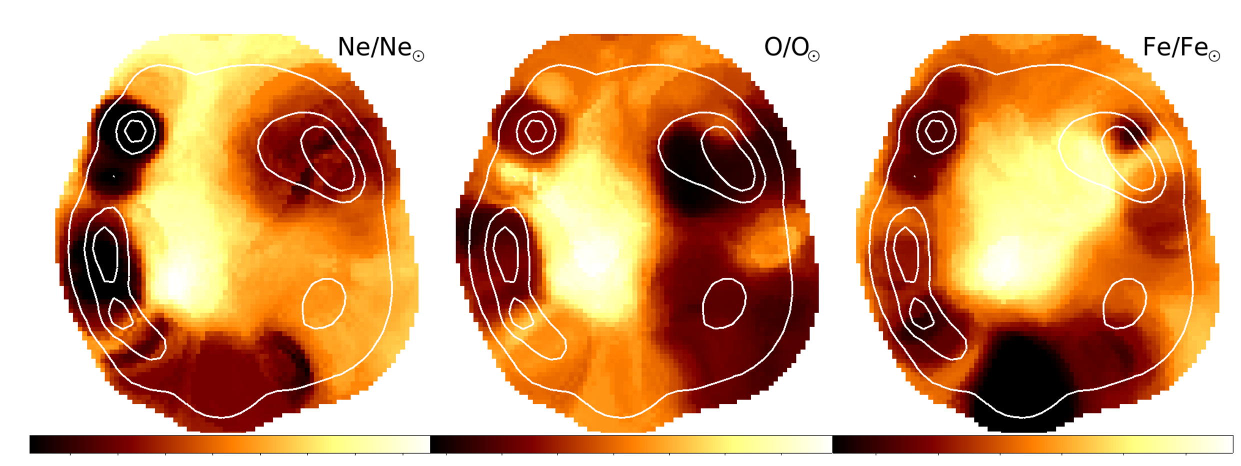

Figure 5: Median EM Weighted Neon (*Left*) Oxygen, (*Center*) and Iron (*Right*) Abundances in Solar [Anders & Grevesse 1989] units.

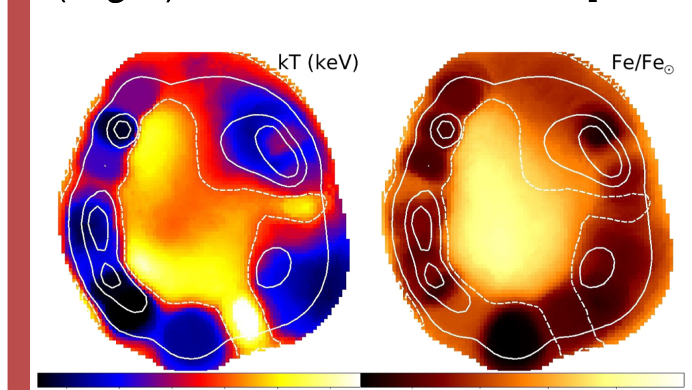

Figure 6: (*Left*) Median Un-weighted Electron Temperature (keV). (*Right*) Unweighted Iron Abundance in Solar (Anders & Grevesse 1989) units.

Note: All contours from the EM map

Abundances

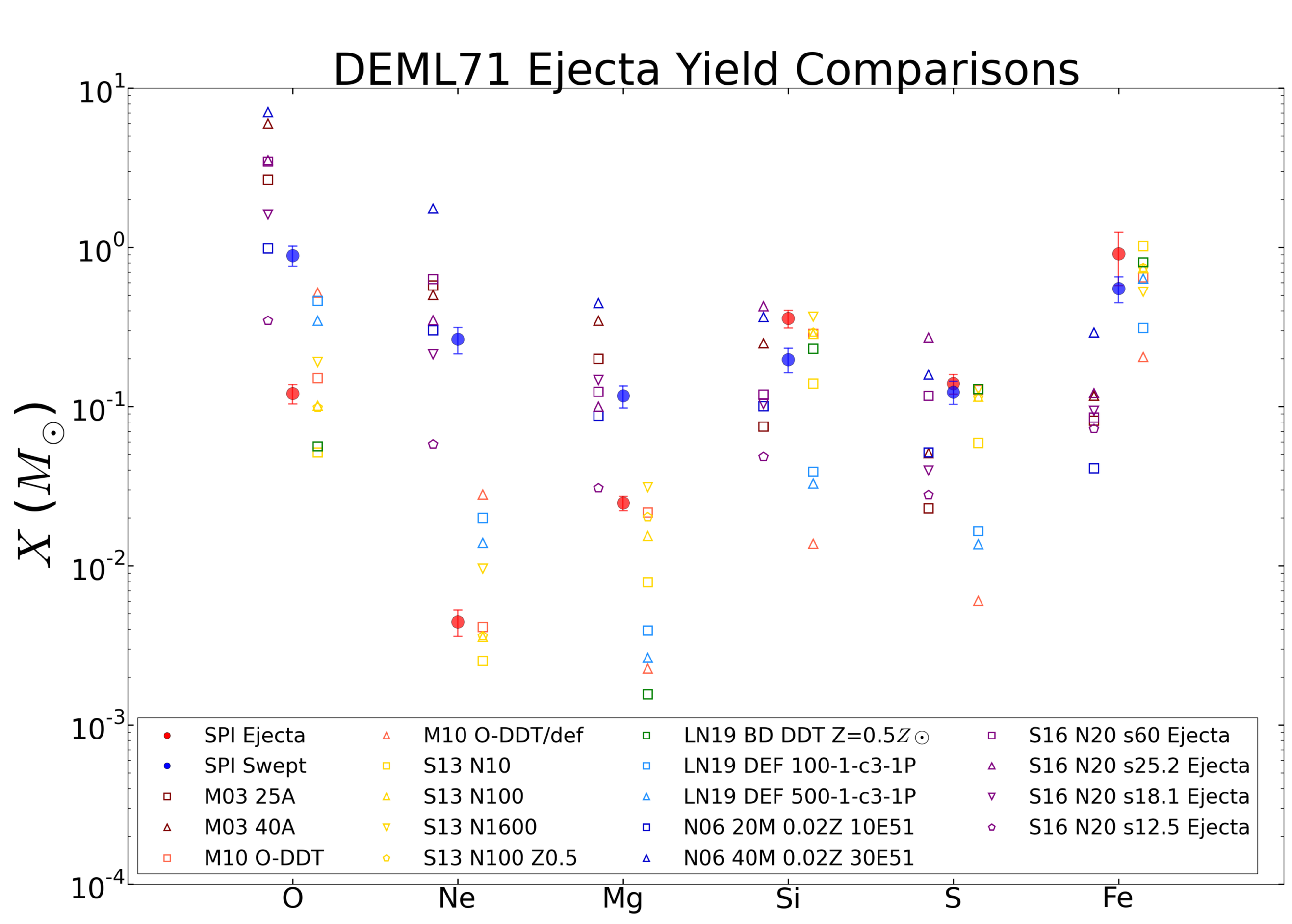

Figure 11: Comparison of ejecta and swept-up abundance with theoretical models for Type Ia and core-collapse explosions.
Red circle – Ejecta, using the Seitenzahl et al (2013) N 100 Z0.5 model, and EM for the isolated ejecta component.
Blue Circle – Swept-up Medium Abundance, from SPI.

References

Anders, E., & Grevesse, N. 1989, GeCoA, 53, 197
Frank, K. A., Dwarkadas, V. V., Panfichi, A., Crum, R. M, & Burrows, D. N, 2019, ApJ, 875, 14
Hughes, J. P., Ghavamian P., Rakowski, C. E., Slane, P., 2003, ApJL, 582, 95
Peterson, J. R., Marshall, P., Andersson, K. E. 2007, ApJ, 655 109
Maggi, P., Haberl, F., Kavanagh, P. J. et al. 2016, A&A, 585, 162
Rakowski, C. E., Ghavamian, P., & Hughes, J. P. 2003, ApJ, 590, 846
Seitenzahl, I. R., Ciaraldi-Schoolman, F., et al. 2013, MNRAS, 429, 1156
van der Heyden, K. J., Bleeker, J. A. M., Kaastra, J. S., Vink, J., 2003, A&A, 406, 141

Conclusions

- Overall, SPI results are consistent with previous work, while highlighting the large range of parameter variations.
- SPI allows for characterization of the plasma properties over the entire remnant volume.
- Enhanced Fe abundance and higher temperature in the core of DEM L71 are consistent with a Type Ia SN origin.
- Using SPI we can identify the contact discontinuity, ejecta, and swept-up region, and analyze the regions individually.